# Pushing the Limit of Infrared Multiphoton Dissociation to Megadalton-Size DNA Ions

**ARTICLE** *in* JOURNAL OF PHYSICAL CHEMISTRY LETTERS · JULY 2012

Impact Factor: 7.46 · DOI: 10.1021/jz300844e



**4 AUTHORS**, INCLUDING:

Tristan Doussineau

**34** PUBLICATIONS **359** CITATIONS

SEE PROFILE

Philippe Dugourd

Claude Bernard University Lyon 1

**207** PUBLICATIONS **3,013** CITATIONS

SEE PROFILE

THE JOURNAL OF PHYSICAL CHEMISTRY Letters

Letter

pubs.acs.org/JPCL

# Pushing the Limit of Infrared Multiphoton Dissociation to Megadalton-Size DNA Ions

Tristan Doussineau, Rodolphe Antoine,* Marion Santacreu, and Philippe Dugourd

Université de Lyon, CNRS, UMR5579, LASIM, Université Lyon 1, Villeurbanne, F-69622 Lyon, France

Supporting Information

**ABSTRACT:** We report the use of infrared multiphoton dissociation (IRMPD) for the determination of relative activation energies for unimolecular dissociation of megadalton DNA ions. Single ions with masses in the megadalton range were stored in an electrostatic ion trap for a few tens of milliseconds and the image current generated by the roundtrips of ions in the trap was recorded. While being trapped, single ions were irradiated by a $CO_2$ laser and fragmented, owing to multiphoton IR activation. The analysis of the single-ion image current during the heating period allows us to measure changes in the charge of the trapped ion. We estimated the activation energy associated with the dissociation of megadalton-size DNA ions in the frame of an Arrhenius-like model by analyzing a large set of individual ions in order to construct a frequency histogram of the dissociation rates for a collection of ions.

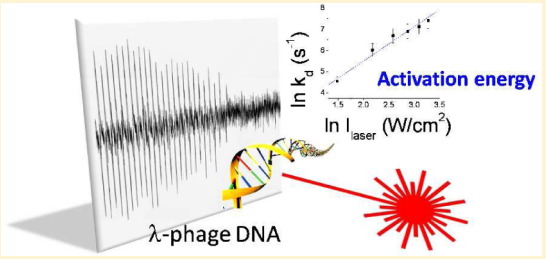


**SECTION:** Biophysical Chemistry and Biomolecules

Manipulation, detection, and spectroscopy at the single-molecule level offer new tools for the study of individual biomolecules under controlled physiological conditions.[1,2] Distributions and time trajectories of physical observables can be measured during a reaction, which has brought new insights into the mechanisms of many processes in molecular biology, including DNA−protein interactions,[3] gene regulation,[4] transcription,[5] translation,[6] and replication.[7] Besides in vitro and in vivo investigations, gas-phase (in vacuo) approaches using ion trapping devices offer the possibility to store and study individual molecules with a well-defined environment. A significant breakthrough was achieved by Whitten and co-workers,[8,9] who pushed detection limits to the single molecule for fluorescent compounds dissolved in macroscopic glycerol−water droplets utilizing ion traps. Fluorescence on single trapped biomolecular ions was demonstrated by Parks and co-workers,[10] for instance. Ion detection at the single-molecule level was pioneered by Smith and co-workers using a Fourier transform ion cyclotron resonance mass spectrometer[11] and by Benner using a charge-detection electrostatic ion trap.[12] These devices allowed the trapping and detection of individual plasmid DNA ions in the megadalton range (i.e., with masses greater than $10^6$ Da). These pioneering works opened the way for the manipulation of single isolated large particles.

Here, we report the use of infrared multiphoton dissociation (IRMPD) for the determination of relative activation energies for unimolecular dissociation of megadalton DNA ions. The single-molecule approach used in this work allows measurement of dissociation rates for individual ions and accumulation of statistics for a collection of ions. Vibrational excitation with IR radiation has been used to study the chemistry of small molecules for decades.[13] McLafferty and co-workers[14] demonstrated the utility of IRMPD for efficient fragmentation of multiply charged ions from proteins and large oligonucleotides.[15] IRMPD with a $CO_2$ laser is exceptionally useful for structural analysis of oligonucleotide and DNA/drug complexes,[16] in large part because of their low bond dissociation energies along the phosphodiester backbone and/or resonance of the photons with P−O stretching frequencies (~1075 $cm^{-1}$ in solution).[17,18] IRMPD can also be used to obtain information about the dissociation energies of ions. The activation energy $E_a$ is obtained from the log-variation of the rate constant against the laser intensity. Although this approach, originally proposed by Dunbar[19] and later refined by Williams and co-workers,[20,21] was successfully applied to polypeptides, the gap to use IRMPD as a tool for probing the energetics of dissociation of large megadalton DNAs has not yet been bridged.

We recently reported the implementation of tandem mass spectrometry for single electrosprayed ions using two charge-detection devices and the coupling with IRMPD using a continuous-wavelength (cw) $CO_2$ laser.[22] Single megadalton ions were stored for several tens of milliseconds. During trapping, single ions were irradiated by the $CO_2$ laser and fragmented following multiphoton IR activation. The analysis of single-ion image current generated by the roundtrips of ions in the trap (wavelets), after a heating period, allows stepwise changes in the charge of the trapped ion to be measured. In this study, we used bacteriophage lambda DNAs (λ-phage DNA). λ-Phage DNA is a linear double-stranded helix containing 48502

**Received:** June 29, 2012
**Accepted:** July 27, 2012
**Published:** July 27, 2012

  

base pairs. Its molecular mass is ~30.6 MDa, and its contour length is ~17.2 $\mu$m.[23] Gas-phase DNA ions were generated by electrospray ionization in positive mode. They were transmitted, selected, and trapped in a charge-detection mass spectrometer used as an electrostatic ion trap (see the Experimental Section). Raw data of charge and mass values recorded for $\lambda$-DNAs are given in Figure S1 (Supporting Information). As already shown by Benner and co-workers,[12,24−26] a broad mass dispersion is observed. It is possible that the ions formed reflect fragmentation as well as clustering of the $\lambda$-DNA during electrospray ionization and transfer to the CD-MS instrument. Experiments were performed on ions with molecular masses close to 30 MDa and a charge of ~1600 e. Figure 1a shows the experimental wavelet created by a single

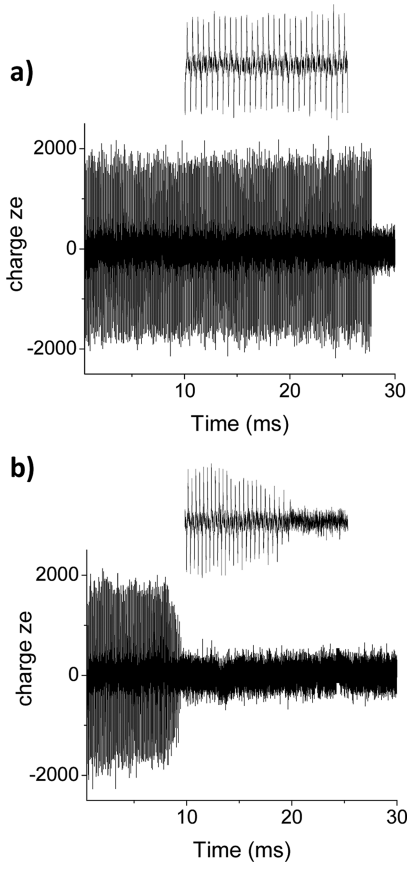


**Figure 1.** (a) Ion wavelet recorded for a single electrosprayed $\lambda$-phage DNA ion stored in the electrostatic ion trap. The inset shows an expanded view of the wavelet from 10 to 12 ms. (b) Ion wavelet recorded for a single electrosprayed $\lambda$-phage DNA ion stored in the electrostatic ion trap under a continuous irradiation of the $CO_2$ laser (14.6 W/cm$^2$). The inset shows an expanded view of the wavelet from 8 to 10 ms. The total charge of the ion gradually decreased before the loss of the particle.

electrospray $\lambda$-phage DNA ion as it traveled back and forth through the ion trap. This single ion was trapped for ~28 ms, during which it cycled ~350 times through the detector tube. Without the laser, individual ions were trapped for ~20−40 ms. No decay in the ion transient over this time was observed, and then, they were suddenly lost, probably due to collision with the neutral molecules. The background gas pressure surrounding the trap was ~3 × $10^{-6}$ mbar for this experiment, corresponding to a collision frequency of ~0.05 per ms.

As the laser is turned on during the ion trapping time, drastic changes are observed both in the trapping duration and the shape of the wavelets. As shown in Figure 1b, under laser irradiation, the trapped ion has a trapping time that does not exceed 10 ms. During the first 8 ms, the amplitude of the charge slightly decreases, as observed in Figure 1b. Then, the amplitude sharply decreases, and for a trapping time longer than 9.5 ms, the particle is no longer detected. During the last step, the total charge is gradually decreased before the ion is lost or cannot be detected (as illustrated in the inset of Figure 1b). In the inset of Figure 1b, just before it is not detected, for each round trip (~79 $\mu$s), the total charge of the ion decreases by ~70 e (~4.4% of the initial total charge). The regular charge loss as a function of time observed after ~8 ms for $\lambda$-phage ions is in favor of sequential losses of bases as compared to the split of the double strand. Successive losses of bases together with a gradual unzipping of the double strand are in agreement with collision-induced dissociation experiments on small DNA strands that lead to the loss of neutral or charged bases.[27,28] The split of the double strand would induce the generation of a fragment ion with a strong reduction of the total charge and a staircase profile for the wavelet (which is not observed here).

Our approach for interpreting the observed kinetics for the dissociation of $\lambda$-phage ions consisted of analyzing a large set of wavelets of individual ions in order to construct a frequency histogram of the distribution of dissociation rates for a collection of ions. Individual trapped ions were irradiated for 48 ms with a laser output power ranging from 10 to 99%. For each laser power, ~100 wavelets of individual ions were analyzed. The normalized ion count at a given time was obtained by the number of traces for which the ion was still detected at this time (ranging from 1 to 30 ms) and, after normalization, over the initial number of traces that was considered.

Figure 2a shows the relative abundance of $\lambda$-phage DNAs as a function of time after $CO_2$ laser irradiation (14.6 W/cm$^2$). The ion count remains approximately constant during an initial induction period (10 ms). This time is required to heat the ions from room temperature to the temperature at which fast dissociation starts. The energetic is measured after the induction time, during which a small monotonic charge loss is observed. This charge loss ranges between 5 and 10% of the initial charge carried by the macroion. Energy that we derived corresponds to dissociation energy, while the $\lambda$-phase DNA has already started to fragment, in particular, after a possible partial unzipping of the double strand. After the induction period, ion dissociation produces a first-order decrease in the parent ion count (straight line in Figure 2b). When increasing laser intensity, the induction time decreases, and the rate of dissociation increases (see Figure 2b). For each laser power, a rate of dissociation is deduced from the linear fit using

$$k_{\mathrm{diss}} = -\frac{\mathrm{d}[\ln(\text{ion count})]}{\mathrm{d}(\text{irradiation time})} \quad (1)$$

Figure 2c displays the evolution of $k_{\mathrm{diss}}$ as a function of the laser intensity in an Arrhenius-like plot. $k_{\mathrm{diss}}$ depends roughly linearly on the laser intensity as a power law

$$\ln k_{\mathrm{diss}} \propto \ln \rho(\nu_{\mathrm{laser}}) \quad (2)$$

In an Arrhenius-like approach, $\ln(k_{\mathrm{diss}})$ is inversely proportional to the temperature. It is not straightforward to analyze experimental results to obtain activation parameters because the

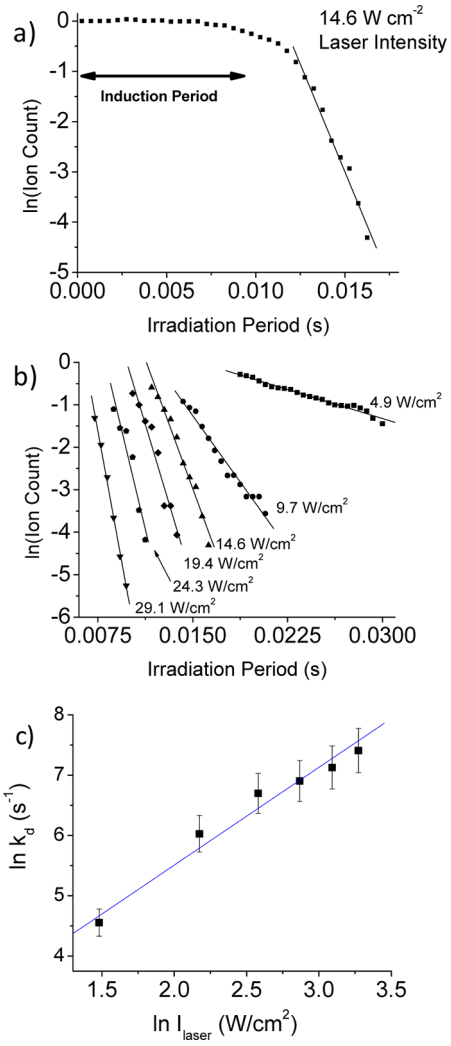


**Figure 2.** (a) Logarithm of ion count versus time for the dissociation of $\lambda$-phage DNA ions under 14.6 W/cm$^2$ $CO_2$ laser irradiation. The plot was constructed by analyzing ~100 wavelets of individual ions at each laser power in order to construct a frequency histogram of the distribution of ion counts (see text for more details). Note the induction time required for the ions to gain sufficiently high internal energy to initiate fast dissociation, after which first-order decay in population is observed. The line corresponds to a linear fit of the data after the induction time. (b) Same as (a) for different laser powers. Data corresponding to the induction time are not shown for clarity. The lines correspond to linear fits of the data. (c) Plot of the logarithm of the first-order unimolecular dissociation rate constant, $k_{diss}$, versus the logarithm of the laser intensity for $\lambda$-phage DNA ions. The activation energy for dissociation, $E_a$, is obtained from the slope of the linear fit (see eqs 4 and 5).

effective temperature of the ions under IR laser irradiation is hard to determine.[29,30] To describe the laser dissociation by simple equations analogous to the Arrhenius equation, a relationship between the laser power and the temperature $T$ of the ions must be derived. Williams and co-workers proposed a model for slow infrared laser dissociation of biomolecules in the rapid energy exchange limit, establishing a relation between the radiation intensity at the laser frequency and temperature[20,21]

$$\frac{\mathrm{d}\ln\rho(\nu_{\mathrm{laser}})}{\mathrm{d}(1/T)} = -s \tag{3}$$

$s$ has units of Kelvins. This model assumes that the ion population reaches a steady state, for which the net absorption is zero in the absence of dissociation.

Substitution of eq 3 directly into the Arrhenius equation $k_{diss} = e^{-E_a/k_bT}$ therefore yields a relationship between the dissociation rate constant and the laser power

$$E_a = sk_b\frac{\mathrm{d}\ln k_{\mathrm{diss}}}{\mathrm{d}\ln\rho(\nu_{\mathrm{laser}})} \tag{4}$$

In this work, we compute $s$ using the IR absorption spectrum of model DNA double strands ($ds(GC)_2$, $ds(GCCG)_2$, and $ds(GCATCG)_2$) calculated at the semiempirical AM1 level (see Figures S2 and S3 and details of the calculations in the Supporting Information). We extracted an average value of $s$ = 2571 K ($s$ = 2476 K for $ds(GC)_2$, $s$ = 2723 K for $ds(GCCG)_2$, and $s$ = 2516 K for $ds(GCATCG)_2$) (close to the value obtained for peptides, i.e., 2675 K). For peptides and proteins, this factor $s$ was found to be constant in the size range of ~0.5−10 kDa.[20,21] Furthermore, $s$ does not depend on the absolute intensity of vibrational transitions but rather depends on the relative intensities of an ion's vibrational transitions (see eq S7 in the Supporting Information). $\lambda$-Phage DNA is a linear double-stranded polymer. The absorption spectrum of linear polymers changes primarily by increasing the number of vibrations as the polymer size increases while not significantly altering the relative absorption intensities. Thus, this factor $s$ is expected to be the same for the entire class of DNAs. We assumed that $s$ was independent of the size of the ion for DNAs, and eq 4 leads to

$$E_a = 0.22\frac{\mathrm{d}\ln k_{\mathrm{diss}}}{\mathrm{d}\ln\rho(\nu_{\mathrm{laser}})} \tag{5}$$

We want to point out that the proportionality constant in eq 5 (0.22) is close to the one derived in the Williams paper (0.23).[21] From the slope of the linear evolution of $k_{diss}$ as a function of laser intensity in a log−log plot (see Figure 2c), one can extract the activation energy for unimolecular dissociation of $\lambda$-phage DNA, $E_a$ = 0.36 ± 0.05 eV.

Blackbody IR dissociation (BIRD) techniques have successfully explored the dissociation of oligonucleotides.[31−35] BIRD dissociations extracted for glycosidic bond and other hydrogen bonds (including Watson−Crick interactions) range between ~1 and 1.7 eV.[31,32] An activation energy of 0.5 eV was reported for the unimolecular dissociation of AATG 16-mer oligonucleotides by IRMPD measurements.[36] These energies are higher than the activation energy reported in this work for $\lambda$-phage DNA. The previous measurements were performed on kDa oligonucleotides composed of dozens of base pairs. A slight decrease in the activation energy was observed as the size of the DNA was increased. The activation energy for unimolecular dissociation of $\lambda$-phage DNA is lower than those reported on small oligonucleotides and confirms that activation energies continue to diminish in large MDa DNA ions. Moreover, we recorded dissociation rates while the DNA had already started to fragment and then probably after partial unzipping of the double strand. The decrease in activation energy could be enhanced by other structural effects. Indeed, the gas-phase linear double-stranded $\lambda$-phage DNA ions may be folded in coiled structures that might induce some torque and constraints on the backbone skeleton, leading to a significant decrease in dissociation energies. Finally, note that the smaller DNA ions studied in previous works by BIRD have charge


dx.doi.org/10.1021/jz300844e | J. Phys. Chem. Lett. 2012, 3, 2141−2145

states between −2 and −3 and $m/z$ values ranging between ∼1000 and 2500. In this study, the average charge state of DNA ions is ∼1600 e, and it corresponds to an average $m/z$ of ∼17500. The charge density of $\lambda$-phage MDa ions is 1 order of magnitude lower than that of the kDa DNA ions studied by BIRD and is not expected to induce significant Coulomb repulsion.

In summary, we reported the use of a cw $CO_2$ laser for the determination of activation energy for unimolecular dissociation of megadalton DNA ions. Single $\lambda$-phage DNA ions were trapped and irradiated with the laser. The analysis of wavelets as a function of time allowed us to extract the dissociation rate constant for several laser intensities. A plot of the logarithm of the first-order rate constant versus the logarithm of the laser intensity yielded a straight line whose slope provided a measure of the activation energy for dissociation. The first assessment of this approach for megadalton-size DNA ions is encouraging, and we hope that IRMPD performed at the single-molecule level will become a successful quantitative method for measuring dissociation energetics for a large panel of nanoobjects.

## EXPERIMENTAL SECTION

The experimental setup consists of a tandem charge-detection mass spectrometer coupled with a cw $CO_2$ laser and is described in details in ref 22. A solution of $\lambda$-phage DNA (Sigma-Aldrich) diluted to 0.0125 g/L (in water/acetonitrile = 50:50 v/v without removing the buffer supplied with the DNA) was electrosprayed in positive mode. Gas-phase ions were transmitted through an ionic train containing a hexapole ion guide and ionic lenses and directed toward the two charge-detection devices (see Figure 3). The first MS stage (first charge-detection device, CDD1) combined with the ion gate (IG) allows $m/z$ and charge selection of a megadalton ion of interest before injection into the ion trap. In this application, when an ion enters the first CDD device, two fast discriminators are used to trigger a transistor−transistor logic pulse based on the voltages induced by the charges ($V_{min} < V < V_{max}$ corresponding to an incoming ion with $Z_{min} < Z < Z_{max}$). The ion gate allowed the selected incoming ion with $Z_{min} < Z < Z_{max}$ to move to the second CDD device (CDD2-IT). When the selected ion enters the second CDD device, it triggers a circuit that enables the potentials on the entrance and exit electrodes to predetermined values designed to reflect ions. During the trapping time, the trapped ions can be fragmented by the IR laser. The laser is a cw $CO_2$ laser ($\lambda$ = 10.6 $\mu$m, output power of 25 W, diameter of 8.1 mm in the trap). The laser beam is reflected by two gold-coated copper mirrors, after which it is injected on the axis of the CDDs through a ZnSe window that is fitted on the rear of the CDD chamber. For laser power dependency experiments, the laser was operated at 5 kHz, and the photon fluence was varied by changing the duty cycle of the laser (from 10 to 99%).

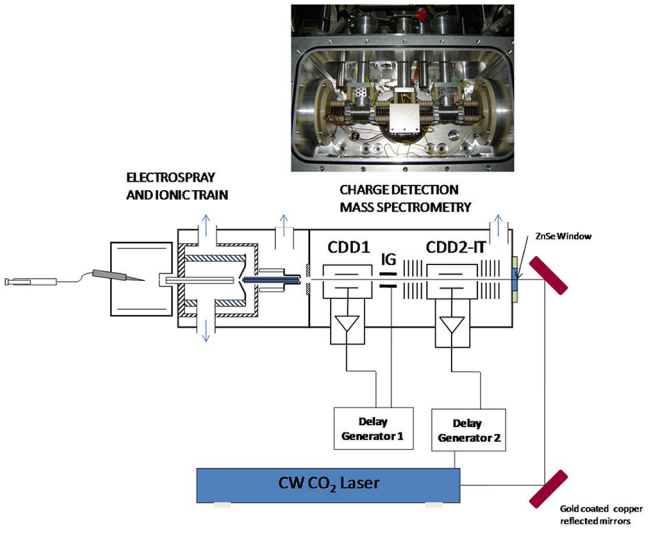


**Figure 3.** Schematic diagram of the experimental setup composed of the electrospray ionization source with the ionic train, the charge-detection devices, and the laser used for photodissociation. The inset shows a photograph of the charge-detection mass spectrometry chamber.

## ASSOCIATED CONTENT

### Supporting Information

Detailed description of Williams's model for IR laser dissociation of large molecules. Raw data of charge and mass values of single ions from electrosprayed $\lambda$-phage DNA. Vibrational frequencies and transitions intensities and the calculated relationship between the relative laser intensity and the ion internal temperature based on AM1-generated frequencies and intensities for model DNA double strands. Charge and time-of-flight precisions in charge-detection mass spectrometry. This material is available free of charge via the Internet at http://pubs.acs.org.

## AUTHOR INFORMATION

### Corresponding Author

*E-mail: rodolphe.antoine@univ-lyon1.fr.

### Notes

The authors declare no competing financial interest.

## ACKNOWLEDGMENTS

We are grateful to the ANR-08-BLAN-0110-01 for financial support of this work. The authors would like to thank Florent Calvo for fruitful discussions and critical comments on the paper. Xavier Dagany, Christian Clavier, Michel Kerleroux, Marc Barbaire, and Jacques Maurelli are acknowledged for their invaluable technical assistance.

## REFERENCES

(1) Mehta, A. D.; Rief, M.; Spudich, J. A.; Smith, D. A.; Simmons, R. M. Single-Molecule Biomechanics with Optical Methods. *Science* **1999**, *283*, 1689−1695.

(2) Weiss, S. Fluorescence Spectroscopy of Single Biomolecules. *Science* **1999**, *283*, 1676−1683.

(3) Gross, P.; Farge, G.; Peterman, E. J. G.; Wuite, G. J. L. Combining Optical Tweezers, Single-Molecule Fluorescence Microscopy, and Microfluidics for Studies of DNA−Protein Interactions. In *Methods in Enzymology, Vol 475: Single Molecule Tools, Pt. B: Super-Resolution, Particle Tracking, Multiparameter, and Force Based Methods*; Elsevier Academic Press Inc: San Diego, CA, 2010; Vol. *474*; pp 427−453.

(4) Raj, A.; van Oudenaarden, A. Single-Molecule Approaches to Stochastic Gene Expression. In *Annual Review of Biophysics*; Annual Reviews: Palo Alto, CA, 2009; Vol. *38*; pp 255−270.

(5) Saleh, O. A.; Allemand, J.-F.; Croquette, V.; Bensimon, D. Single-Molecule Manipulation Measurements of DNA Transport Proteins. *ChemPhysChem* **2005**, *6*, 813−818.

(6) Munro, J. B.; Sanbonmatsu, K. Y.; Spahn, C. M. T.; Blanchard, S. C. Navigating the Ribosome's Metastable Energy Landscape. *Trends Biochem. Sci.* **2009**, *34*, 390−400.
(7) van Oijen, A. M.; Loparo, J. J. Single-Molecule Studies of the Replisome. In *Annual Review of Biophysics*; Annual Reviews: Palo Alto, CA, 2010; Vol. *39*; pp 429−448.
(8) Whitten, W. B.; Ramsey, J. M.; Arnold, S.; Bronk, B. V. Single-Molecule Detection Limits in Levitated Microdroplets. *Anal. Chem.* **1991**, *63*, 1027−1031.
(9) Barnes, M. D.; Ng, K. C.; Whitten, W. B.; Ramsey, J. M. Detection of Single Rhodamine 6g Molecules in Levitated Microdroplets. *Anal. Chem.* **1993**, *65*, 2360−2365.
(10) Iavarone, A. T.; Duft, D.; Parks, J. H. Shedding Light on Biomolecule Conformational Dynamics Using Fluorescence Measurements of Trapped Ions. *J. Phys. Chem. A* **2006**, *110*, 12714−12727.
(11) Smith, R. D.; Cheng, X.; Bruce, J. E.; Hofstadler, S. A.; Anderson, G. A. Trapping, Detection and Reaction of Very Large Single Molecular-Ions by Mass-Spectrometry. *Nature* **1994**, *369*, 137−139.
(12) Benner, W. H. A Gated Electrostatic Ion Trap to Repetitiously Measure the Charge and m/z of Large Electrospray Ions. *Anal. Chem.* **1997**, *69*, 4162−4168.
(13) Dunbar, R. C. New Approaches to Ion Thermochemistry Via Dissociation and Association. In *Advances in Gas Phase Ion Chemistry*; Babcock, L. M., Adams, N. G., Eds.; JAI Press: Greenwich, CT, 1996; Vol. 2; p 87.
(14) Little, D. P.; Speir, J. P.; Senko, M. W.; Oconnor, P. B.; McLafferty, F. W. Infrared Multiphoton Dissociation of Large Multiply-Charged Ions for Biomolecule Sequencing. *Anal. Chem.* **1994**, *66*, 2809−2815.
(15) Little, D. P.; Aaserud, D. J.; Valaskovic, G. A.; McLafferty, F. W. Sequence Information from 42−108-Mer DNAs (Complete for a 50-Mer) by Tandem Mass Spectrometry. *J. Am. Chem. Soc.* **1996**, *118*, 9352−9359.
(16) Brodbelt, J. S.; Wilson, J. J. Infrared Multiphoton Dissociation in Quadrupole Ion Traps. *Mass Spectrom. Rev.* **2009**, *28*, 390−424.
(17) Wang, L.; Yang, L.; Keiderling, T. A. Vibrational Circular Dichroism of A-, B-, and Z-Form Nucleic Acids in the Po2-Stretching Region. *Biophys. J.* **1994**, *67*, 2460−2467.
(18) Banyay, M.; Sarkar, M.; Graslund, A. A Library of IR Bands of Nucleic Acids in Solution. *Biophys. Chem.* **2003**, *104*, 477−488.
(19) Dunbar, R. C. Kinetics of Low-Intensity Infrared-Laser Photodissociation — The Thermal-Model and Application of the Tolman Theorem. *J. Chem. Phys.* **1991**, *95*, 2537−2548.
(20) Paech, K.; Jockusch, R. A.; Williams, E. R. Slow Infrared Laser Dissociation of Molecules in the Rapid Energy Exchange Limit. *J. Phys. Chem. A* **2002**, *106*, 9761−9766.
(21) Paech, K.; Jockusch, R. A.; Williams, E. R. Slow Infrared Laser Dissociation of Biomolecules in the Rapid Energy Exchange Limit. *J. Phys. Chem. A* **2003**, *107*, 2596−2596.
(22) Doussineau, T.; Bao, C. Y.; Clavier, C.; Dagany, X.; Kerleroux, M.; Antoine, R.; Dugourd, P. Infrared Multiphoton Dissociation Tandem Charge Detection-Mass Spectrometry of Single Megadalton Electrosprayed Ions. *Rev. Sci. Intrum.* **2011**, *82*, 084104.
(23) Sanger, F.; Coulson, A. R.; Hong, G. F.; Hill, D. F.; Petersen, G. B. Nucleotide Sequence of Bacteriophage Lambda DNA. *J. Mol. Biol.* **1982**, *162*, 729−773.
(24) Fuerstenau, S. D.; Benner, W. H. Molecular Weight Determination of Megadalton DNA Electrospray Ions Using Charge Detection Time-of-Flight Mass Spectrometry. *Rapid Commun. Mass Spectrom.* **1995**, *9*, 1528−1538.
(25) Schultz, J. C.; Hack, C. A.; Benner, W. H. Mass Determination of Megadalton-DNA Electrospray Ions Using Charge Detection Mass Spectrometry. *J. Am. Soc. Mass Spectrom.* **1998**, *9*, 305−313.
(26) Schultz, J. C.; Hack, C. A.; Benner, W. H. Polymerase Chain Reaction Products Analyzed by Charge Detection Mass Spectrometry. *Rapid Commun. Mass Spectrom.* **1999**, *13*, 15−20.
(27) Wu, J.; McLuckey, S. A. Gas-Phase Fragmentation of Oligonucleotide Ions. *Int. J. Mass Spectrom.* **2004**, *237*, 197−241.
(28) Gabelica, V.; Tabarin, T.; Antoine, R.; Rosu, F.; Compagnon, I.; Broyer, M.; Pauw, E. D.; Dugourd, P. Electron Photodetachment Dissociation of DNA Polyanions in a Quadrupole Ion Trap Mass Spectrometer. *Anal. Chem.* **2006**, *78*, 6564−6572.
(29) Dunbar, R. C. BIRD (Blackbody Infrared Radiative Dissociation): Evolution, Principles, and Applications. *Mass Spectrom. Rev.* **2004**, *23*, 127−158.
(30) Laskin, J.; Futrell, J. H. Activation of Large Ions in FT-ICR Mass Spectrometry. *Mass Spectrom. Rev.* **2005**, *24*, 135−167.
(31) Klassen, J. S.; Schnier, P. D.; Williams, E. R. Blackbody Infrared Radiative Dissociation of Oligonucleotide Anions. *J. Am. Soc. Mass Spectrom.* **1998**, *9*, 1117−1124.
(32) Schnier, P. D.; Klassen, J. S.; Strittmatter, E. F.; Williams, E. R. Activation Energies for Dissociation of Double Strand Oligonucleotide Anions: Evidence for Watson−Crick Base Pairing In Vacuo. *J. Am. Chem. Soc.* **1998**, *120*, 9605−9613.
(33) Strittmatter, E.; Schnier, P.; Klassen, J.; Williams, E. Dissociation Energies of Deoxyribose Nucleotide Dimer Anions Measured Using Blackbody Infrared Radiative Dissociation. *J. Am. Soc. Mass Spectrom.* **1999**, *10*, 1095−1104.
(34) Daneshfar, R.; Klassen, J. Arrhenius Activation Parameters for the Loss of Neutral Nucleobases from Deprotonated Oligonucleotide Anions in the Gas Phase. *J. Am. Soc. Mass Spectrom.* **2004**, *15*, 55−64.
(35) Daneshfar, R.; Klassen, J. Thermal Decomposition of Multiply Charged T-Rich Oligonucleotide Anions in the Gas Phase. Influence of Internal Solvation on the Arrhenius Parameters for Neutral Base Loss. *J. Am. Soc. Mass Spectrom.* **2006**, *17*, 1229−1238.
(36) Hannis, J. C.; Muddiman, D. C. Tailoring the Gas-Phase Dissociation and Determining the Relative Energy of Activation for Dissociation of 7-Deaza Purine Modified Oligonucleotides Containing a Repeating Motif. *Int. J. Mass Spectrom.* **2002**, *219*, 139−150.